Master QLMN Antoine Browaeys
Experimental quantum computing antoine.browaeys@institutoptique.fr

Lecture 3 - Optical qubits

January 14th 2026

Light, and in particular its constituent the photon, looks like a good candidate to store quantum information. There are several attractive features in favor of using light to encode qubits. First, as it travels at the speed of light, it is the qubit of choice for communication and hence to interconnect quantum processors. Second, light propagates with nearly no absorption in many materials: for example the attenuation in optical fiber is 0.2-0.3 dB/km at telecom wavelengths, meaning that "T_1 can be long". Also the polarization for the light can be maintained quite well (meaning "long T_2"). More generally, photons are quite immune to electromagnetic perturbations. Third, from a technological point of view, integrated photonics is well developed at the industry level, thus facilitating the transition towards industrial photonic quantum processor, when the route finally becomes clear.

There are two ways to store qubits on light. The first one relies on single photons and requires single-photon sources and detectors. The second uses weak coherent pulses and manipulates the quadratures of the field. Both approaches face however the same difficulty: photons interact only very weakly, making it challenging to build entangling gates. We will see in this lecture how to circumvent this problem.

Despite this main difficulty, several companies follow the optical approach such as Quandela (France), PsiQuantum (USA) and Xanadu (Canada). Today, they often define the state-of-the art for the performances of the hardware, but a lot of academic research explores the many open questions remaining to be solved for the photonics approach.

1 Linear optics quantum computing using single photons [1]

We start by the first approach relying on single photons, assuming that we have all the necessary hardware (see Sec. 3). This first approach makes use only of linear optical elements, and the non-linearity necessary for entangling operations is provided by a measurement: it leads to a non-linear update of the photon wavefunction and acts as an effective photon-photon interaction.

Qubit encoding. They are two standard ways to encode the qubit on a photon (see Fig. 1). The first one uses the two orthogonal polarizations perpendicular to the wavevector $\mathbf{k}$, for example $|0\rangle = |H\rangle, |1\rangle = |V\rangle$ (polarization encoding). The second one, convenient in particular when using integrated photonics technology, relies on two paths (propagation modes) a and b of the photon: $|0\rangle = |n_a = 0, n_b = 1\rangle$ and $|1\rangle = |n_a = 1, n_b = 0\rangle$, where $n_{a,b}$ are the number of photons in the modes a, b (dual rail encoding).

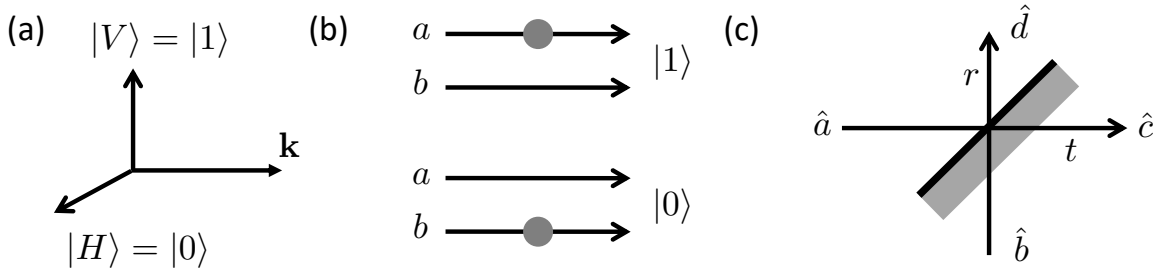

Figure 1: *(a) Polarization and (b) dual rail encoding. (c) Action of a beamsplitter.*

Exercise 1. Use a polarization beamsplitter to show how to convert the polarization encoding into a dual-rail encoding and vice-versa.

Beamsplitters and phase shifters. These are the main linear components used in optics. The beamsplitter BS (transmission and reflection coefficients t, r) implements the unitary transformation $\hat{U}_{\rm BS}$ of the input modes a, b into the output modes c, d in the following way (Fig. 1c):

$$\begin{pmatrix} \hat{c} \\ \hat{d} \end{pmatrix} = \hat{U}_{\rm BS} \begin{pmatrix} \hat{a} \\ \hat{b} \end{pmatrix} \quad \text{with} \quad \hat{U}_{\rm BS} = \begin{pmatrix} t & -r \\ r & t \end{pmatrix} \quad \text{or} \quad \hat{U}_{\rm BS} = \begin{pmatrix} t & ir \\ ir & t \end{pmatrix} \ . \tag{1}$$

with $\hat{a}, \hat{b}, \hat{c}, \hat{d}$ the corresponding annihilation operators obeying the commutation rules $[\hat{a}, \hat{a}^+] = [\hat{b}, \hat{b}^+] = [\hat{c}, \hat{c}^+] = [\hat{d}, \hat{d}^+] = 1$ and any cross commutators, e.g., $[\hat{a}, \hat{c}^+] = 0$. Energy conservation imposes $|r|^2 + |t|^2 = 1$. Several conventions are possible for $\hat{U}_{\rm BS}$, as shown above. A phase plate implements the following operation:

$$\hat{U}(\phi) = \begin{pmatrix} 1 & 0 \\ 0 & e^{i\phi} \end{pmatrix} \ . \tag{2}$$

Let us recall the action of a 50/50 beamsplitter on two important states of the field. First, a single photon in mode a, with no photon in mode b:

$$|1_a, 0_b\rangle = \hat{a}^+ |0, 0\rangle = \frac{1}{\sqrt{2}}(\hat{c}^+ + \hat{d}^+) |0, 0\rangle = \frac{1}{\sqrt{2}}(|1_c, 0_d\rangle + |0_c, 1_d\rangle) \ . \tag{3}$$

This operation entangles the modes c, d (yes... with just one photon...). If two identical photons arrive on the BS, one in each input port, we obtain:

$$|1_a, 1_b\rangle = \hat{a}^+\hat{b}^+ |0, 0\rangle = \frac{1}{\sqrt{2}}(\hat{c}^+ + \hat{d}^+)\frac{1}{\sqrt{2}}(\hat{c}^+ - \hat{d}^+) |0, 0\rangle = \frac{1}{\sqrt{2}}(|2_c, 0_d\rangle - |0_c, 2_d\rangle) \ . \tag{4}$$

This is the Hong-Ou-Mandel effect that you have seen in Quantum Optics.

Single qubit gates. Combining BS and phase shifters allows one to perform any single-qubit operation using the dual rail encoding. For the polarization encoding, one

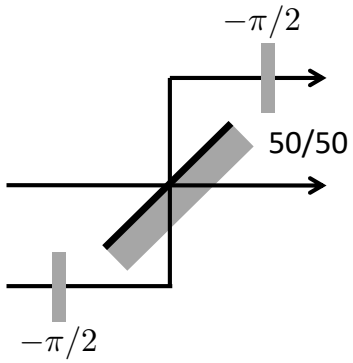

Figure 2: *Optical setup implementing a Hadamard gate in the dual rail encoding. The grey rectangles represent phase shifters with* $\phi = -\pi/2$.

simply uses a half waveplate oriented with an angle θ with respect to the horizontal axis, which performs the unitary transform:

$$\hat{U}_{\text{pol}} = \begin{pmatrix} \cos\theta & \sin\theta \\ \sin\theta & -\cos\theta \end{pmatrix} . \tag{5}$$

Exercise 2. Show that the setup in Fig. 2 implements a Hadamard gate in the dual rail encoding. Use the second convention in (1) for $\hat{U}_{\text{BS}}$.

Probabilistic two-qubit gates. This is where the difficulty lies, as photon in free space do not interact. We use instead of the interaction a measurement, which ensures a non-linear update of the wavefunction. The price to pay is that the approach is now *probabilistic*. The general framework was introduced in 2001 by Knill, Laflamme and Milburn [3] and we summarize it below.

First, we construct a non-linear phase shifter which applies the following transformation:

$$|\psi_{\text{in}}\rangle = \alpha\,|n=0\rangle + \beta\,|n=1\rangle + \gamma\,|n=2\rangle \to |\psi_{\text{out}}\rangle = \alpha\,|n=0\rangle + \beta\,|n=1\rangle - \gamma\,|n=2\rangle \ , \tag{6}$$

i.e. we flip the sign of the state when two photons are in the same mode. To implement this transformation, we use the optical setup represented in Fig. 3(a): it requires two auxiliary qubits in modes a, b, on top of the initial state we want to act on. One of them is in state $|1\rangle$, the second one in $|0\rangle$. Two detectors A and B are placed at the output. When detector A clicks, it heralds the preparation of $|\psi_{\text{out}}\rangle$, i.e. the successful operation of the non-linear shifter. To understand how this works, we consider separately the cases where $|\psi_{\text{in}}\rangle$ contains either 0, 1 or 2 photons.

When $|\psi_{\text{in}}\rangle = |n=0\rangle$, the only way to obtain a click on detector A and no click on B is that the photon a has either been reflected on BS1, BS2 and BS3, which occurs with an amplitude $\sqrt{R_1R_2R_3}$, or that it is transmitted by BS1 and BS3 (amplitude $\sqrt{(1-R_1)(1-R_3)}$). The amplitude corresponding to a click is thus $C_0 = \sqrt{R_1R_2R_3} + \sqrt{(1-R_1)(1-R_3)}$. When instead $|\psi_{\text{in}}\rangle = |n=1\rangle$, a click on detector A only corresponds to the amplitude $C_1 = -\sqrt{R_2}(\sqrt{R_1R_2R_3} + \sqrt{(1-R_1)(1-R_3)}) + (1-R_2)\sqrt{R_1R_3}$.

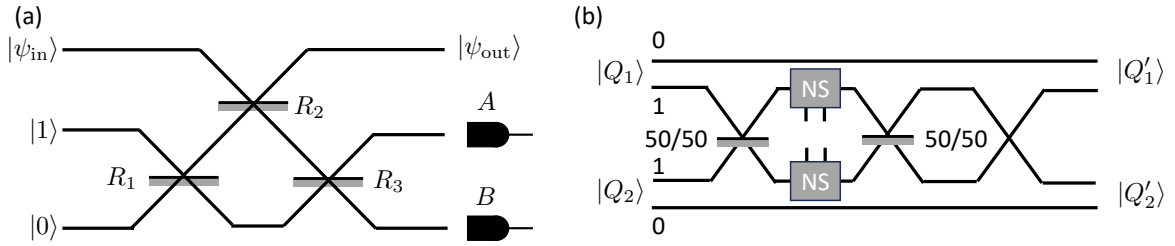

Figure 3: *(a) Optical setup implementing the non-linear shifter (NS). Here R_i are the reflection coefficient in intensity. (b) Setup to implement a probabilistic CZ gate.*

Finally for $|\psi_{\rm in}\rangle = |n=2\rangle$, a click on detector A only corresponds to the amplitude $C_2 = R_2(\sqrt{R_1R_2R_3} + \sqrt{(1-R_1)(1-R_3)}) - 2\sqrt{R_2}(1-R_2)\sqrt{R_1R_3}$. The non-linear shifting operation imposes $C_0 = C_1 = -C_2 = C$ and a tedious calculation yields $R_2 = (\sqrt{2}-1)^2$. The largest value of C is obtained for $R_1 = R3 = (4-2\sqrt{2})^{-1}$. It gives the upper limit for the probability of success of the shifter, $p = C^2 = 1/4$.

Exercise 3. Explain how you get the expression of C_1 and C_2. If you have some courage calculate R_2, and $R_1 = R_3$.

This non-linear phase shifter is now used to implement a probabilistic CZ gate with the circuit shown in Fig. 3(b).

Exercise 4. By considering the action of the circuit on each of the state $|0,0\rangle$, $|0,1\rangle$, $|1,0\rangle$, and $|1,1\rangle$ show that it implements a CZ phase gate $|Q_1,Q_2\rangle \to (-1)^{Q_1+Q_2}|Q_1,Q_2\rangle$. Be careful with the definition of the modes carrying 0 and 1. For the BS, take:

$$\hat{U}_{\rm BS} = \frac{1}{\sqrt{2}}\begin{pmatrix} 1 & i \\ i & 1 \end{pmatrix} . \tag{7}$$

As the circuit involves two non-linear shifters, the probability of success is $p = (1/4)^2 = 1/16$. This of course makes the realization of a long circuit unpractical, as the probability of getting the result after the application of N gates is p^N. The KLM framework proposes a solution to this problem.

The KLM approach. It relies on near deterministic gate teleportation. As a reminder (see Lecture 3 from course on Physics of Quantum Information), teleportation consists in sending a qubit $|\psi\rangle_A = \alpha|0\rangle + \beta|1\rangle$ between two partners Alice (A) and Bob (B) by performing a measurement followed by a classical transmission from A to B. More precisely, A and B share a Bell pair encoded on two photons 2 and 3, for example: $|\phi_-\rangle_{23} = (|01\rangle_{23} - |10\rangle_{23})/\sqrt{2}$. Alice performs a Bell measurement (see below) between her qubit in $|\psi\rangle_A$ and photon 2. She gets one of the following results (m,n): (11), (10), (01) or (00) corresponding to each of the Bell states:

$$|\phi_+\rangle_{12} = (|01\rangle_{12} + |10\rangle_{12})/\sqrt{2}\ ,\ |\phi_-\rangle_{12} = (|01\rangle_{12} - |10\rangle_{12})/\sqrt{2}\ ,$$
$$|\psi_+\rangle_{12} = (|00\rangle_{12} + |11\rangle_{12})/\sqrt{2}\ ,\ |\psi_-\rangle_{12} = (|00\rangle_{12} - |11\rangle_{12})/\sqrt{2}\ .$$

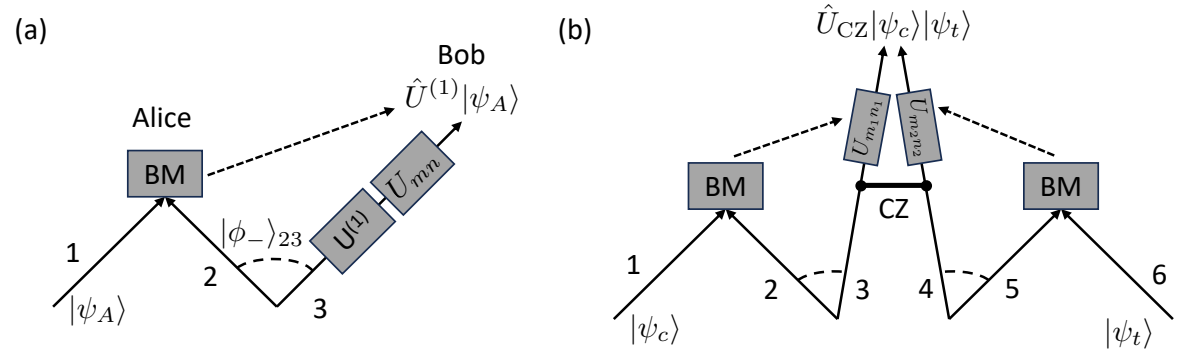

Figure 4: *(a) Sigle-qubit gate teleportation. (b) CZ gate teleportation.*

Alice then sends the result (m, n) to Bob, who applies a unitary operation $\hat{U}_{mn}$ to his qubit, in order to restore the initial state of Alice's qubit on his own qubit now encoded on photon 3.

$$\hat{U}_{11} = \hat{XZ}, \hat{U}_{01} = \hat{Z}, \hat{U}_{10} = \hat{X}, \hat{U}_{00} = \hat{\mathbb{1}} \ .$$

Teleporting a single-qubit gate means that if you apply on photon 3 the unitary operation $\hat{U}^{(1)}$, Bob's qubit will be in the state $X^m Z^n \hat{U}^{(1)} |\psi_A\rangle$ (see Fig. 4a).

Teleporting a two-qubit gate is more involved and relies on the scheme shown in Fig. 4(b). You want to apply a two-qubit gate between photons without having them interact: photon 1 encodes the control qubit $|\psi_c\rangle$ and 6 carries $|\psi_t\rangle$. You need as a resource two pairs of entangled photons. You apply the two-qubit gate (here a CZ) between photon 3 and 4, and then apply the unitaries $\hat{U}_{m_1,n_1}$ and $\hat{U}_{m_2,n_2}$. The end result is that the photons 3 and 4 have undergone the CZ gate and are in the state $\hat{U}_{\rm CZ}|\psi_c\rangle|\psi_t\rangle$. Of course the CZ gate between the resource photons 3 and 4 is probabilistic. However, you perform the teleportation only when the heralding signal tells you that the CZ is successful. Only then do you teleport the states: you apply the two Bell measurements and send the classical signal. The CZ gate now becomes deterministic: the probabilistic aspect, still present, comes from the "off-line resources" (the two Bell states) that do no contribute directly. The two photons 3 and 4 that have undergone the teleported gate can now be used in a next CZ gate by the same mechanism. In order for the scheme to work you do need however some delay lines or means to store photons $|\psi_c\rangle$, $|\psi_t\rangle$, 1-4 so that when the CZ is successful, you have the time perform the Bell measurements followed by the teleportation.

Everything seems alright: we have a way to apply sequential CZ or CNOT gates in a deterministic way, albeit at the price of preparing extra resources (the Bell pairs). The only problem is that the Bell measurement has a success probability of 1/2 as it is not able to distinguish between the states $|\psi_+\rangle$, $|\psi_-\rangle$...

Exercise 5. The Bell measurement setup is shown in Fig. 5(a) for the dual rail encoding. Show that it allows distinguishing between states $|\psi_+\rangle$, $|\psi_-\rangle$ but not between $|\phi_+\rangle$ or $|\phi_-\rangle$. Calculate the probability of success.

Exercise 6. Same question for the polarization encoding, with the setup shown in

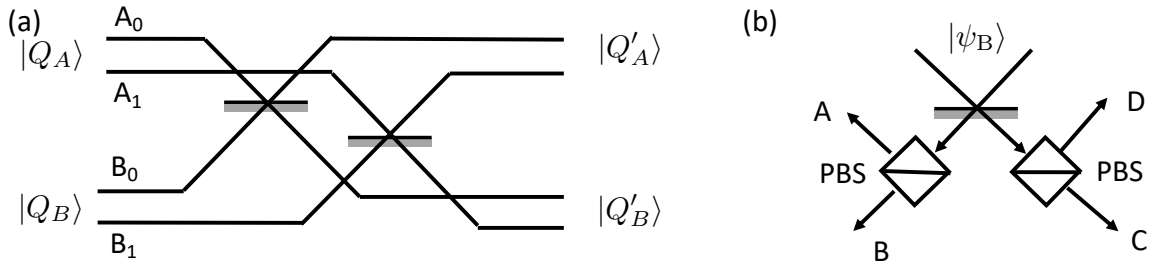

Figure 5: *(a) Optical setup implementing a Bell measurement in the dual rail encoding. (b) Bell measurement in the polarization encoding.*

Fig. 5(b).

The probability of success of the teleported CNOT gate is thus $(1/2)^2 = 1/4$ as it involves the teleportation of two qubits, and it looks like we are back to the initial problem of probabilistic gate. However, KLM proposed a method to make the Bell measurement probability arbitrary close to 1 by using n auxiliary photons prepared in a state $|t_n\rangle$. The exact way of doing this is quite involved and we will not detail it, but they calculate a success probability of the Bell measurement of $n/(n+1)$, meaning that using these extra photons, the probability of the CNOT gate is now $p_{\text{CNOT}} = [n/(n+1)]^2$. For example, for $n = 2$, you would need 2 photons in 4 auxiliary modes (dual rail encoding) in the state $|t_2\rangle = (|1100\rangle + |1010\rangle + |1001\rangle)/\sqrt{3}$. If you want a fidelity $p_{\text{CNOT}} = 0.99$, you need 200 auxiliary photons (prepared in a very specific state)!

Measurement based quantum computing approach. As shown above, the KLM protocol is very greedy in terms of resources. In 2001, Robert Raussendorf and Hans J. Briegel, proposed a different approach, called measurement based quantum computing (MBQC) [4]. It relies on a resource state (called cluster state or graph state) which features entanglement between the qubits. A given quantum algorithm is now a sequence of measurements on each qubit sequencially, where the result s_i at step i fixes the measurement one has to perform at step $i+1$ (adaptative measurement). The result of the algorithm is then given by the last measurement, and at the end of the sequence the cluster state is destroyed. In this approach no gate is applied on the qubits, and one relies only on a deterministic sequence of measurements which depend on the algorithm. However, the construction of the cluster state in the photonic approach is, so far, probabilistic, as we detail below.

The authors of Ref. [4] showed that any single-qubit gates and a CNOT gate can be generated in this way, thus ensuring the equivalence between MBQC and the traditional gate based model. Let us first show that we can implement any single qubit operator of the form $\hat{U}(\alpha, \beta, \gamma) = \mathcal{R}_x(\alpha).\mathcal{R}_z(\beta).\mathcal{R}_x(\gamma)$ using the MBQC approach. We rely on 5 qubits, initially prepared in the state $|\psi_1\rangle \otimes |+\rangle_2 \otimes |+\rangle_3 \otimes |+\rangle_4 \otimes |+\rangle_5$, where $|\psi_1\rangle$ is the qubit we want $\hat{U}$ to act on. To prepare the cluster state, we apply CZ gates between each adjacent qubits. The sequential measurement of each qubit is done in the $|\pm\rangle_\theta = (|0\rangle \pm e^{i\theta}\ |1\rangle)/\sqrt{2}$ basis. If the result of the measurement on qubit j gives $|+\rangle_j$,

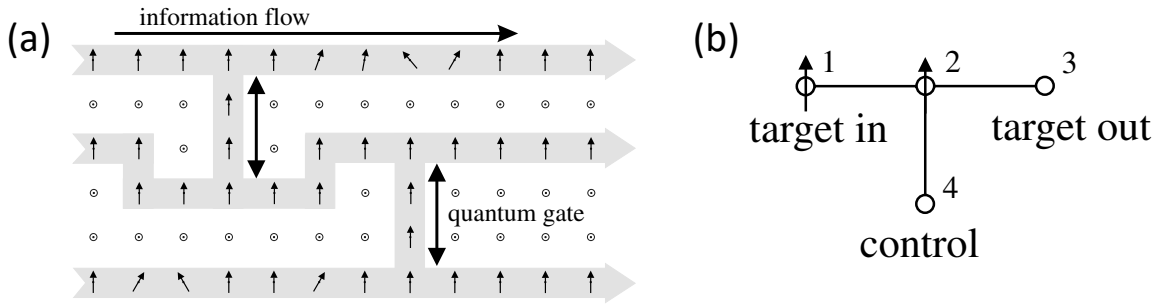

Figure 6: *(a) Principle of MBQC where a sequence of measurement and feedforward implements a given algorithm. (b) CNOT gate in the MBQC approach. From [4].*

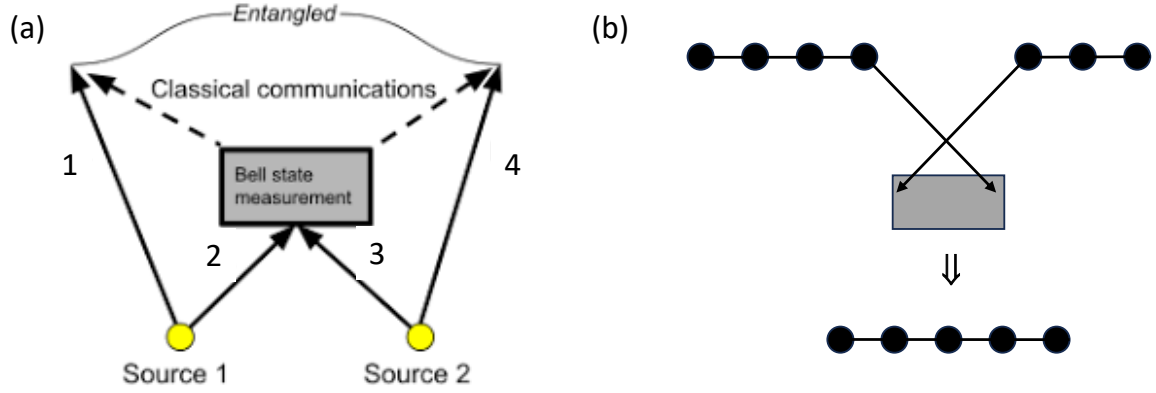

Figure 7: *(a) Principle of entanglement swapping by Bell measurement. (b) Fusion of two entangled states to generate a larger one.*

then $s_j = 0$, and $s_j = 1$ otherwise: this is the result of the measurement which we use to define the one at step $j+1$. The sequence is then the following: (1) measure qubit 1 with $\theta_1 = 0$. The result is s_1; (2) measure qubit 2 with $\theta_2 = (-1)^{s_1}\alpha$, and get s_2; (3) measure qubit 3 with $\theta_3 = (-1)^{s_2}\beta$, and get s_3; (4) measure qubit 4 with $\theta_4 = (-1)^{s_1+s_3}\gamma$ and get s_4. At the end, the qubit 5 is projected onto the state $|\psi_5\rangle = \hat{X}^{s_2+s_4}\hat{Z}^{s_1+s_3}U(\alpha,\beta,\gamma)\,|\psi_1\rangle$.

To realize a CNOT gate between 2 qubits, one uses a cluster state containing 4 qubits arranged as shown in Fig. 6. Prepare first the state $|i\rangle_1\,|j\rangle_4\,|+\rangle_2\,|+\rangle_3$, where $i,j \in 0,1$ are the states of the control and target qubits. Then apply the CZ gates between all the connected pairs to obtain the cluster state. Read out sequentially 1,2,3 and 4 and get each time the result s_n. At the end of the sequence, you find that qubit 3 is in the state $|i_1 \oplus i_4\rangle_3$ and thus carries the results of the CNOT gate between qubit 1 (control) and 4 (target).

The cluster state is usually hard to write explicitly when the number of qubits is large. However the procedure to construct it is easy to define: one simply apply CZ gate between adjacent qubits, as show in the examples above. The cluster state is universal, in the sense that any algorithm can be run using the same state. However, its construction is probabilistic in the photonic approach, as the CZ gate is probabilistic.

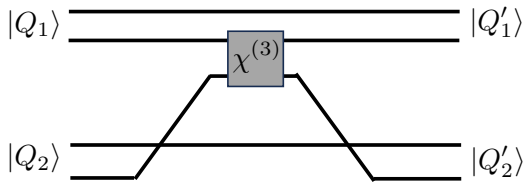

Figure 8: *Principle of a gate based on the Kerr effect in dual rail encoding.*

In the photon based quantum computing community, a lot of research is dedicated today to devise efficient construction scheme of the cluster state. A popular approach relies on fusion gates, whose basic ingredient is entanglement swapping, which we now describe. The procedure is shown in Fig. 7(a): you start from two Bell states $|\psi_{12}\rangle$ and $|\psi_{34}\rangle$ and perform a Bell measurement on photons 2 and 3. Depending on the outcome of the measurement, the photons 1 and 4 are now entangled in a specific Bell state.

Exercise 7. Show that this is the case. Take $|\psi_{12}\rangle = |\psi_+\rangle_{12}$ and $|\psi_{34}\rangle = |\psi_+\rangle_{34}$. Calculate the success probability.

Fusion gates are the generalization of entanglement swapping when the two states to be combined are not simply Bell states, but more complicated ones such as GHZ with more than 3 photons. The generic scheme is shown in Fig. 7(b). Cluster states of up to 6 photons have been recently demonstrated, with a success rate of 2 mHz (1 state generated every 500 sec) [5].

As a conclusion of this first section, the linear approach to optical quantum computing faces a significant challenge in scaling up, owing to its probabilistic nature. This is the reason why a lot of research is also devoted to making photons interact deterministically, as we now discuss.

2 Non-linear optics quantum computing with single photons

In this second approach, we go back to the traditional gate based circuit model and rely on a direct photon-photon interaction to build deterministic gates. Such interaction can be obtained in a non-linear medium, for example one exhibiting Kerr non-linearity. In the dual rail encoding, a phase gate corresponds to the scheme represented in Fig. 8. The action of the Kerr non-linearity is represented by the Hamiltonian $H_{\text{Kerr}} = \hbar\phi\,\hat{n}_1\hat{n}_2$, where $\hat{n}_i = \hat{a}_i^+\hat{a}_i$ is the photon number operator. The unitary evolution of the state $|Q_1, Q_2\rangle$ is set by the length L of the Kerr medium and the phase velocity v_φ of the photons propagating through it, yielding $\hat{U} = \exp[-iH_{\text{Kerr}}L/v_\varphi]$.

To relate the phase ϕ to the non-linear properties of the medium, recall that the non-linear polarization for a Kerr medium is related to the linear and non-linear sus-

ceptibilities $\chi^{(1,3)}$ by

$$P = \epsilon_0 \chi^{(1)} E + \epsilon_0 \chi^{(3)} |E|^2 E + ... \tag{8}$$

The index of refraction is thus for $\chi \ll 1$

$$n = \sqrt{1+\chi} \approx 1 + \frac{\chi}{2} = 1 + \frac{\chi^{(1)}}{2} + \frac{\chi^{(3)}}{2} E_1 E_2 \tag{9}$$

where E_1 and E_2 are the amplitude of the field associated to the two interacting photons (cross-Kerr effect). Hence the non linear phase is

$$\phi = 2\pi \frac{\chi^{(3)}}{2} E_1 E_2 \frac{L}{\lambda} \ .$$

Everything looks good, apart form the fact that the values of the $\chi^{(3)}$ coefficient of most Kerr media are very small: In $LiNbO_3$, $\chi^{(3)} \sim 10^{-21}$ m^2/V^2; for organic polymers $\chi^{(3)} \sim 10^{-16}$ m^2/V^2 and for the largest reported values in atomic medium in an electromagnetically induced transparency (EIT) condition, $\chi^{(3)} \sim 10^{-7}$ m^2/V^2. To get an estimate of the phase ϕ that these non-linearities lead to, we calculate the field of a single photon in the following way: $\hbar\omega = \epsilon_0 c E^2 \pi w^2 L_c$, where w is the radius of the cylindrical mode we suppose the photon to be in, and L_c is the coherence length of the photon, which depends on the source generating it. Taking as a source an atom or a quantum dots with a decay time $\tau_c \approx 10\,\text{ns}$ yields $L_c \approx c\tau_c \approx 3\,\text{m}$. For a wavelength around $1\,\mu$m, we obtain $E \approx 3$ V/m and $\phi \sim 10^{-10}$ in a polymer. Hence usual non-linearities are too weak to envision using them to build a phase gate.

Two main ideas have been proposed, and partially demonstrated, to enhance optical non-linearities using either a cavity QED approach or an Rydberg interaction induced non-linearity.

The CQED approach. Here, the general framework is the Jaynes-Cumming model describing a two-level atom (states $|g\rangle, |e\rangle$, transition frequency ω_0) coupled to the optical mode of a cavity (frequency ω_c). Recall that for a detuning $\Delta = \omega_c - \omega_0$ and a single-photon Rabi frequency Ω_1, the Hamiltonian in the rotating wave approximation is

$$H_{\text{JC}} = \frac{\hbar\Delta}{2}\hat{\sigma}_z + \hbar\Omega_1(\hat{\sigma}^+\hat{a} + \hat{\sigma}^-\hat{a}^+) \quad \text{with} \quad \hbar\Omega_1 = d_{eg}\sqrt{\frac{\hbar\omega_c}{2\epsilon_0 V}} \ . \tag{10}$$

The eigenenergies and corresponding eigenstates of the coupled atom-field system are

$$E_+(n) = \hbar\sqrt{\frac{\Delta^2}{4} + \Omega_1^2 n} \quad \text{with} \ |n,+\rangle = \cos\frac{\theta}{2}|g,n\rangle + \sin\frac{\theta}{2}|e,n-1\rangle \ ; \tag{11}$$

$$E_-(n) = -\hbar\sqrt{\frac{\Delta^2}{4} + \Omega_1^2 n} \quad \text{with} \quad |n,-\rangle = -\sin\frac{\theta}{2}|g,n\rangle + \cos\frac{\theta}{2}|e,n-1\rangle \ , \tag{12}$$

where n is the number of photons in the mode and $\tan\theta = 2\Omega_1\sqrt{n}/\Delta$. Let us consider the dispersive regime where $|\Delta| \gg \Omega_1\sqrt{n}$. A Taylor expansion of the energy yields

$$E_+(n) \approx \frac{\hbar\Delta}{2} + \frac{\hbar\Omega_1^2}{\Delta}n - \frac{\hbar\Omega_1^4}{\Delta^3}n^2 \quad \text{and} \quad |n,+\rangle \approx |g,n\rangle \ . \tag{13}$$

The last term ressembles the Kerr non-linearity we are looking for. Hence, the phase difference accumulated for a state containing $n = 1$ or $n = 2$ photons is

$$\phi = (E_+(2) - 2E_+(1))t/\hbar = -\frac{2\Omega_1^4}{\Delta^3}t \ . \tag{14}$$

Taking $\Omega_1/(2\pi) = 1$ MHz, $\Delta = 10\Omega_1$ and an interaction time $t = 1\,\mu$s, we get $\phi = \pi$, just what we need to build a CZ gate. The key ingredient that we used here is the anharmonic spectrum of the Jaynes-Cumming model. For the above argument to be valid though, we need to work in the so-called strong coupling regime $\Omega_1^2/(\kappa\Gamma) \gg 1$, where κ is the cavity linewidth and Γ is the linewidth of the atomic transition.

Non-linearity induced by Rydberg interactions. The principle of this non-linearity combines Electromagnetically Induced Transparency with the Rydberg blockade that we studied in Lecture 2. It uses a cloud of atoms (usually laser-cooled, for example here Rb) with density $\mathcal{N}$ and involves three atomic levels $|g\rangle$, $|e\rangle$ and $|r\rangle$ in a ladder configuration, as represented in Fig. 9. The low transition has a wavelength of 780 nm (D2 line of Rb), and the higher one 480 nm. Here $|r\rangle$ is a Rydberg state. The Rabi frequency on the $e-r$ transition is Ω_c and dominates all the other (control field). The signal field on the $g-e$ transition will be the one containing either 1 or 2 photons. We work here in the dispersive regime of EIT to illustrate the working mechanism, i.e. we set $\omega_c + \omega_s = \omega_{gr}$, but the fields are detuned by Δ with respect to the state $|e\rangle$. If the signal field contains only one photon, it goes through the medium without acquiring a phase: this comes from the fact that the index of refraction of a medium at an EIT condition is zero, and the transmission is 1. If now two photons are in the signal field, the first one excites an atom to the Rydberg state: this shifts the energy level of all the atoms in a sphere of radius $R_b = (C_6/\Omega)^{1/6}$ (Rydberg blockade). Thus the EIT condition is no longer fulfilled for all these atoms and the second photon travelling in the blockade sphere, with a frequency detuned by Δ with respect to the $e-g$ transition, sees a medium consisting of two-level atoms only, as the $e-r$ transition is now irrelevant. The phase accumulated during its propagation is thus

$$\phi = \frac{k_{780}}{2}\chi_{2\text{lvl}}R_b \quad \text{with} \quad \chi_{2\text{lvl}} \approx \mathcal{N}\frac{6\pi}{k^3}\frac{\Gamma}{\Delta} \ . \tag{15}$$

Introducing the optical depth $\text{OD}_b = \mathcal{N}6\pi/k^2R_b$, we find $\phi = \text{OD}_b\Gamma/\Delta$. If we take realistic values for $R_b = 5$ (corresponding to a Rydberg state $60S$), $\text{OD}_b = 10$ and $\Gamma/\Delta = 0.1$ we obtain $\phi \sim \pi$. If the principle exposed above is correct, the detailed analysis is significantly more involved: one has to take into account the propagation of the light pulse associated to a single photon in the medium and its conversion into so-called dark state polariton propagating at the group velocity.

The idea of combining EIT with Rydberg interactions was proposed and demonstrated in 2008 by C.S. Adams at Durham university (UK). Recent demonstrations of Rydberg-induced phase gate lead to fidelities around 40%, and are usually obtained by placing the atomic cloud in an optical cavities. A lot of research is still necessary to make this approach fully functional.

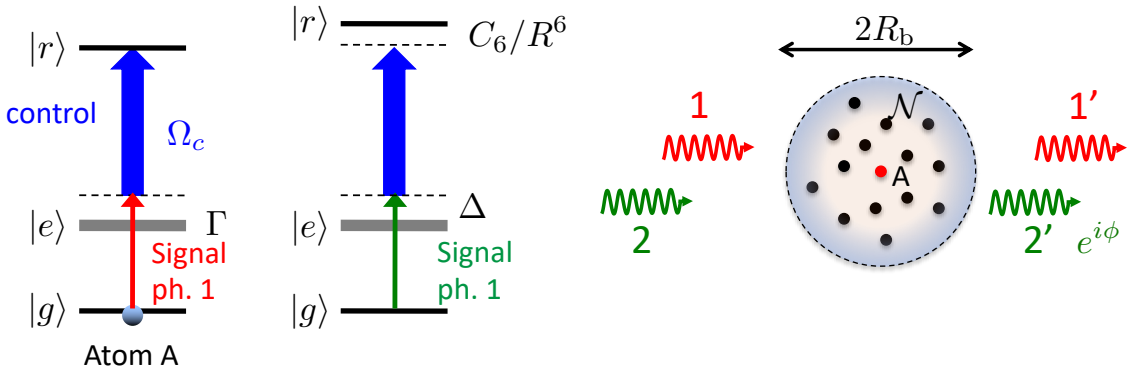

Figure 9: *Principle of a non-linearity combining Electromagnetically Induced Transparency and Rydberg interaction.*

3 Hardware for single photon based quantum computing

The linear and non-linear approaches to discrete optical quantum computing require: (1) a source of identical single photons with a high flux; (2) high efficiency single photon detectors; (3) beamsplitters; (4) waveplates, phase shifters, modulators...

For the two last items, one has to distinguish lab experiments that usually rely on bulk free space optics, while the industry rather uses fully fibered or integrated optics solution. For example, beamsplitters, modulators or polarization control devices exist in fibered versions, and are highly efficient especially at telecom wavelength as used everywhere in communication technologies. Here we concentrate on what remains a challenge today: the source and the detector.

Single-photon sources. There are two kinds of sources; the first one relies on spontaneous parametric down-conversion where a pump laser at frequency ω_p propagating in a $\chi^{(3)}$ medium generates photon pairs $|n_a = 1, n_b = 1\rangle$ in two modes a and b, with frequencies $\omega_{a,b}$ fulfilling $\omega_p = \omega_a + \omega_b$. The wavevectors must satisfy the phase matching condition $\mathbf{k}_p = \mathbf{k}_a + \mathbf{k}_b$. Other higher order non-linear processes are also possible like spontaneous four wave mixing. In this scheme, one of the two photons is detected and the positive detection in, say, mode b heralds the presence of a single photon in a, thus the name *heralded single photon source*. More precisely, the $\chi^{(3)}$ non-linear medium is described by the Hamiltonian

$$H = \hbar\chi(\hat{a}^+\hat{b}^+ + \hat{a}\hat{b})I_p \tag{16}$$

with I_p the pump laser power. Its action on the vacuum state $|0_a, 0_b\rangle$ gives

$$|\psi_{ab}\rangle \approx |0_a, 0_b\rangle + \epsilon\,|1_a, 1_b\rangle + \epsilon^2\,|2_a, 2_b\rangle + ... \tag{17}$$

with $\epsilon \propto I_p$. This indicates that pumping harder leads to unwanted pairs of pairs, and therefore there is a limit to the flux of emitted single photons. In practice it is less

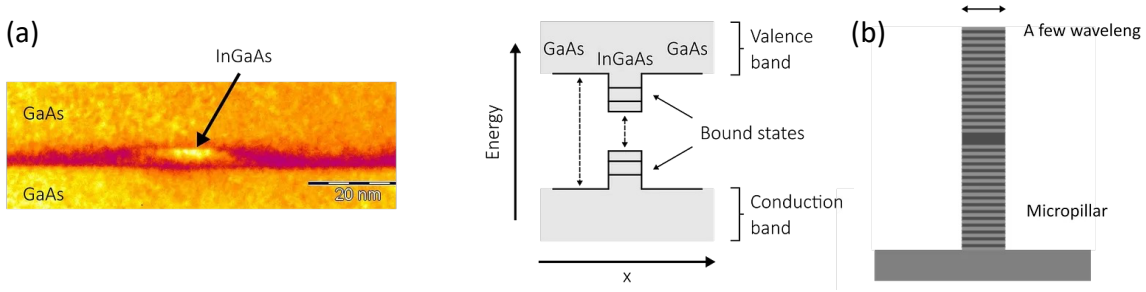

Figure 10: *(a) Quantum dots as a single photon emitter. (b) Cavity made of Bragg mirrors into which the quantum dots is placed. Figures from [7].*

than $\sim 10^7$/s. A nice feature though is the easy integration of these type of source on photonic chips. The american company PsiQuantum uses this technology.

The second type of source is in principle deterministic: it is based on individual quantum emitters like atoms or ions, or solid state emitters (NV centers or quantum dots). Let us describe the quantum dots approach used in particular by the french company Quandela. It relies on building a three dimensional semi-conductor structure that acts as an essentially infinite potential well for the electrons. The structure is obtained by inserting InAs into GaAs which have different band gaps (around 1 eV). The dot is excited by laser pulses and photons are emitted at a wavelength around 900 nm. However the emission occurs in a large solid angle, resulting into a low collection efficiency. The way around consists in placing the quantum dots inside a cavity made of high reflectivity Bragg mirrors. The Purcell effect enhances the emission in the mode of the cavity by a factor $\beta = F_p/(1+F_p)$, where $F_p = (3/4\pi^2)(\lambda/n)^3(Q/V)$ with n the index of refraction of the material, V the volume of the cavity and Q its quality factor. The photons coming out of the cavity in a given direction can then be efficiently coupled to a fiber. Quandela obtains in this way rate of single photons around 80 MHz, and the efficiency of the source is 65%.

Exercise 8. Quandela measured a reduction of the lifetime of the quantum dots from 1.3 ns in free-space to 160 ps when placed in the cavity. The emission wavelength is 890 nm. Calculate the Purcell factor F_p. If the quality factor is $Q = 12000$, estimate the volume of the cavity. The index of refraction of the material is $n \approx 3.5$. Calculate β. Why is the efficiency only 65%?

To quantify how close a given source is to an ideal single photon source, one uses the intensity correlation function (in steady-state)

$$g^{(2)}(\tau) = \frac{\langle \hat{a}^+(t)\hat{a}^+(t+\tau)\hat{a}(t+\tau)\hat{a}(t)\rangle}{\langle \hat{a}^+\hat{a}\rangle^2} \,. \tag{18}$$

This quantity counts the number of coincides one obtains at time t and $t+\tau$. A good single photon source should have $g^{(2)}(0) \approx 0$. To measure it, one implements the optical setup shown in Fig. 11: during a time bin Δt, one measures the number of coincidences N_c obtained on the two detectors, and normalize by the number of

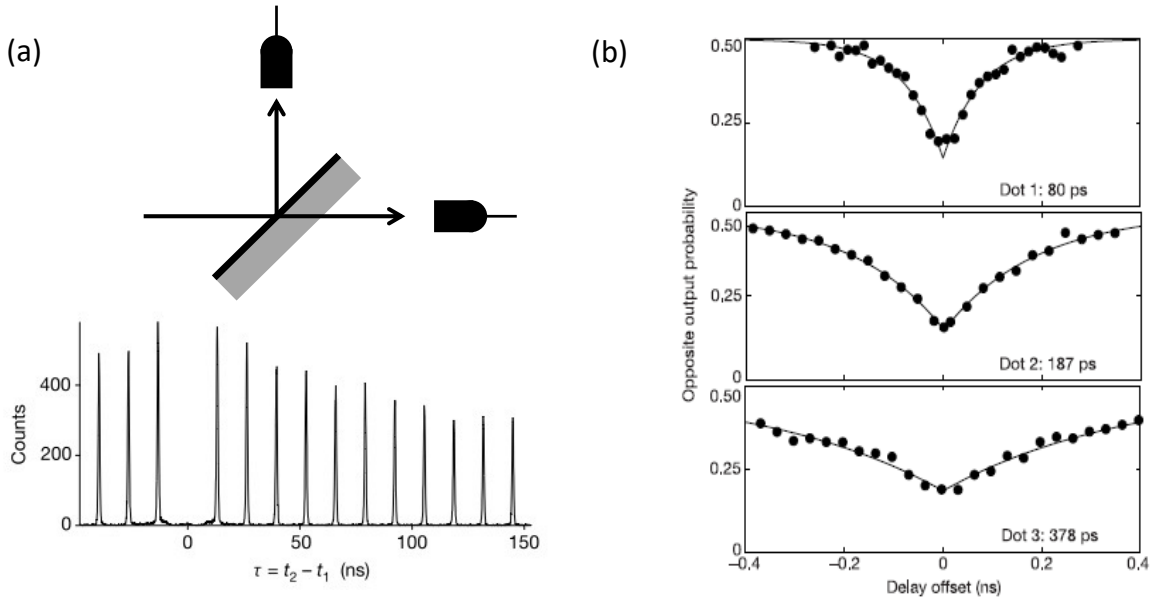

Figure 11: *(a) Hanbury-Brown and Twiss setup and measured $g^{(2)}(0)$ for a quantum dot photon source. (b) Examples of HOM signal for three different quantum dots source. Figures from [6].*

counts $N_{1,2}$ on each arms during the same time bin. Then $g^{(2)}(0) = N_c/(N_1 N_2)$. Quandela obtains $g^{(2)}(0) < 0.01$ with its quantum dots source, while PsiQuantum reports $g^{(2)}(0) = 3 \times 10^{-3}$.

Exercise 9. Show that $g^{(2)}(0) = 2P_2/P_1^2$, where $P_{1,2}$ is the probability that the field contains 1 or 2 photons. How much is it for a weak coherent pulse?

Exercise 10. Calculate $g^{(2)}(0)$ for the single photon state in mode a resulting from the heralding on mode b of the state (17) produced by spontaneous downconversion.

The second important property of the source is how identical the emitted photons are. As we saw in the linear quantum computing approach, an essential ingredient is the Hong-Ou-Mandel two-photon interference on a beamsplitter. Preparing the state (4) requires the two photons at the input of the beamsplitter to be exactly in the same spatio-temporal mode. If this is not the case, the output state will have a small detrimental $|1_c, 1_d\rangle$ contribution. One can describe the temporal mode of the field into which a two-level emitters emits a single photon by the function $E(t) = e^{-\Gamma t/2}\, e^{-i\omega_0 t}$, where Γ is the linewidth of the transition and ω_0 its frequency. If for any reason ω_0 fluctuates (phonons for a solid state emitters for example), the photons will not all be produced in the same temporal mode. To quantify this, we delays one photon with respect to a following one and we count the number of coincidences obtained on detectors c, d. It should be close to zero for nearly identical photons, due to the HOM effect. Examples are shown in Fig. 11(b). In practice one rather quotes the contrast of the "HOM dip". Quandela reports 94% for a source operating at 5K to reduce the influence of phonon induced dephasing, and PsiQuantum gives 99.5%. Reference [7] gives a nice introduc-

tion to single photon sources and their characterization.

Single-photon detectors. Before 1980's, most of the single photon counters used in quantum optics were photomultiplier tubes, with poor quantum efficiency in the IR. In the 80's people started to use single photon avalanche photodiodes (SPAD) that are semi-conducting PN junction inversely polarized. A photon propagating through the central part will be absorbed and create an electron which is accelerated by the inverse voltage up to a kinetic energy large enough to ionize surrounding atoms. It generates an avalanche of electrons, which is then stopped by an appropriate circuit lowering the inverse voltage. A single photon therefore generates a pulse of charges of a few ns which is easily detected. The quantum efficiency of these detectors is above 50% in the visible for Si-based versions. They usually feature a dead-time of about 10 ns following the detection of a photon, during which it cannot detect another one. Besides, it cannot resolve the number of photons.

More recently appeared photon number resolving detectors based on superconducing nanowires (SNSPD). The idea is to run a current through the superconducting wires maintained just above the critical current. When a photon is absorbed somewhere on the wire it locally heats it, and the current has to be concentrated outside this region, thus increasing the current density above its critical value: the whole wire becomes resistive and the voltage across the wire increases sharply. Adjusting the critical current allows one to resolve up to 5 photons. These detectors are however less handy to use and require a closed circuit of liquid He to maintain the superconductivity of the wires.

4 Continuous variable quantum computing

We finish off this overview of optical qubits by mentioning very briefly the continuous variable approach, which is a world in itself. It relies on weak coherent pulses of light, i.e. attenuated laser beams, easier to generate than single photons. The price to pay is the difficulty to perform the single and two-qubit gates.

Recall that the mode of an electromagnetic fields is equivalent to a harmonic oscillator, and therefore can contain an infinite number of excitations. Coherent states are superposition of photon number states $|n\rangle$. The electric field operator $\hat{E}$ can be written in terms of its quadratures $\hat{X}$ and $\hat{P}$ as:

$$\hat{E} = \mathcal{E}_v(\hat{X}\cos\omega t + \hat{P}\sin\omega t) \quad \text{with} \quad [\hat{X},\hat{P}] = i \ , \tag{19}$$

and where $\mathcal{E}_v = \sqrt{\hbar\omega/(2\epsilon_0 V)}$. A coherent state is represented in phase space by an arrow featuring a blurring end to indicate the intrinsic vacuum fluctuations resulting from $\Delta P \Delta X \geq 1/2$ (Fig. 12a).

There are several ways to encode qubits. The first one consists in encoding on coherent states with opposite phase: $|0\rangle = |\alpha\rangle$ and $|1\rangle = |-\alpha\rangle$(Fig. 12a). This qubit is quite robust to bit flip errors, whose probability is reduced by $\langle -\alpha|\alpha\rangle \sim \exp(-2|\alpha|^2)$. Performing a single qubit gate like the Hadamard gate is however challenging, as it

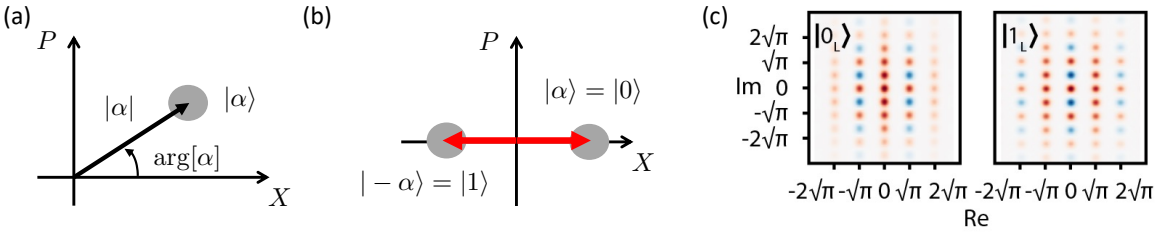

Figure 12: *(a) Phase space representation of a coherent state. (b) Qubit encoding on two coherent states. (c) Phase space representation of a GKP state.*

amounts to preparing Schrödinger cat states

$$|\pm\rangle = \frac{1}{\sqrt{2(1 \pm |\alpha|^2)}}(|\alpha\rangle + |-\alpha\rangle) \ . \tag{20}$$

This can be done but requires using non-linear media which generate optical squeezing and conditional measurements. Two qubit gates are also possible

The second type of encoding also aims at being more resilient to errors and uses the idea of logical encoding that we will explore i n more details in the last part of the course on quantum error correction. Popular states are Gottesman, Knill, Preskill (GKP) states:

$$|0\rangle_{\rm L} = \sum_n |X = 2n\sqrt{\pi}\rangle \quad ; \quad |1\rangle_{\rm L} = \sum_n |X = (2n+1)\sqrt{\pi}\rangle \ . \tag{21}$$

In phase space, they correspond to a grid, as shown in Fig. 12(c). One can show that gaussian operations (e.g. rotations in phase space, squeezing of the quadrature...) applied to GKP states allows for universal quantum computing. The first experimental demonstration of (small...) GKP states in optics is recent and requires a source of squeezed vacuum, beam splitter and conditional measurements. [9].

Although continuous variable quantum computing is actively explored in optics, today it is much more advanced in circuit QED using microwave photons, as we will see in Lecture 4.

References

[1] P. Kok *et al.*, "Linear optical quantum computing", Rev. Mod. Phys. **79**, 135 (2007).

[2] Janos A. Bergou, Mark Hillery, Mark Saffman, Quantum Information Processing: Theory and Implementation, Springer (2021).

[3] E. Knill, R. Laflamme and G. J. Milburn, "A scheme for efficient quantum computation with linear optics", Nature **409**, 46 (2001).

[4] E. Knill, R. Laflamme and G. J. Milburn, "A One-Way Quantum Computer", Phys. Rev. Lett. **86**, 5188 (2001).

[5] V. Guichard *et al.*, "Monitoring the generation of photonic linear cluster states with partial measurements", Quantum Sci. Technol. **11**, 015015 (2025).

[6] C. Santori *et al.*, "Indistinguishable photons from a single-photon device", Nature **419**, 594 (2001)

[7] Quandela: Single photon sources.

[8] Xin Zhang *et al.*, "Universal control of four singlet-triplet qubits", Nature Nanomaterial **20**, 209 (2025).

[9] S. Konno *et al.*, "Propagating Gottesman-Kitaev-Preskill states encoded in an optical oscillator", Science **383**, 289 (2023).